Cork Open Research Archive
Cartlann Taighde Oscailte Chorcaí

Title	Formation of nanoporous InP by electrochemical anodization
Author(s)	Buckley, D. Noel; O'Dwyer, Colm; Lynch, Robert P.; Newcomb, Simon B.
Publication date	2004-01
Original citation	Buckley, D. N., O'Dwyer, C., Lynch, R., Sutton, D., Newcomb, S. B. (2004) 'Formation of Nanoporous InP by Electrochemical Anodization', 206th Meeting of the Electrochemical Society: State -of-the-Art Program on Compound Semiconductors XLI. Hilton Hawaiian Village, Honolulu, Hawaii, 3-8 October. Pennington, NJ: The Electrochemical Society, 6, pp. 103-117.
Type of publication	Conference item
Rights	
Item downloaded from	http://hdl.handle.net/10468/1011

University College Cork, Ireland
Coláiste na hOllscoile Corcaigh

FORMATION OF NANOPOROUS INP BY ELECTROCHEMICAL ANODIZATION

D.N. Buckley[†‡], C. O'Dwyer[†‡Θ], R. Lynch[†‡], D. Sutton[‡#] and S.B. Newcomb[‡*]

[†]*Department of Physics, University of Limerick, Ireland*
[‡]*Materials & Surface Science Institute, University of Limerick*
[Θ]*present address: Université Paul Sabatier, Toulouse, France*
[*]*present address: Sonsam Ltd., Glebe Laboratories, Newport, Co. Tipperary, Ireland*
[#]*present address: Limerick Institute of Technology, Ireland*

ABSTRACT

Porous InP layers can be formed electrochemically on (100) oriented n-InP substrates in aqueous KOH. A nanoporous layer is obtained underneath a dense near-surface layer and the pores appear to propagate from holes through the near-surface layer. In the early stages of the anodization transmission electron microscopy (TEM) clearly shows individual porous domains which appear to have a square-based pyramidal shape. Each domain appears to develop from an individual surface pit which forms a channel through this near-surface layer. We suggest that the pyramidal structure arises as a result of preferential pore propagation along the <100> directions. AFM measurements show that the density of surface pits increases with time. Each of these pits acts as a source for a pyramidal porous domain. When the domains grow, the current density increases correspondingly. Eventually, the domains meet forming a continuous porous layer, the interface between the porous and bulk InP becomes relatively flat and its total effective surface area decreases resulting in a decrease in the current density. Numerical models of this process have been developed. Current-time curves at constant potential exhibit a peak and porous layers are observed to form beneath the electrode surface. The density of pits formed on the surface increases with time and approaches a plateau value.

INTRODUCTION

There is considerable interest in the electrochemical formation of porosity in semiconductors, both from the point of view of fundamental understanding and their applications. [1-7] Much of the work has focused on silicon but investigations of pore formation in III-V semiconductors such as GaAs [8-11] and InP [12-15] have also been reported. It has been suggested that controlled modulation of the pore diameter and pore growth direction in such structures could lead to photonic crystals with a photonic band gap in the near infra-red or visible region. These characteristics are affected by electrolyte concentration [12,16,17], substrate type [18], orientation [19] and doping

density. [20] Significant progress has been made in understanding the basic mechanisms of pore formation in silicon under electrochemical conditions, but only a limited number of investigations of the mechanism of pore formation in III-V semiconductors have been reported. For silicon, several pore formation models have been proposed to account for the variety of observed pore types [21-23]. In this paper we review our recent work on the formation of porous InP during anodization in KOH electrolytes.

EXPERIMENTAL

The working electrode consisted of polished (100)-oriented monocrystalline sulfur doped n-InP with a carrier concentration of $\sim 3 \times 10^{18}$ cm^{-3}. An ohmic contact was made by alloying indium to the InP sample and the contact was isolated from the electrolyte by means of a suitable varnish. The electrode area was typically 0.2 cm^2. Anodization was carried out in an aqueous KOH electrolyte at a concentration of 5 mol dm^{-3}. A conventional three electrode configuration was used employing a platinum counter electrode and saturated calomel reference electrode (SCE) to which all potentials are referenced. Prior to immersion in the electrolyte, the working electrode was dipped in a 3:1:1 H_2SO_4:H_2O_2:H_2O etchant and rinsed in deionized water. All of the electrochemical experiments were carried out at room temperature and in dark conditions.

A CH Instruments Model 650A Electrochemical Workstation interfaced to a Personal Computer (PC) was employed for cell parameter control and for data acquisition. Slices for plan view and cross-sectional microscopic analysis were prepared by thinning to electron transparency using standard focused ion beam milling procedures by means of a FEI 200 FIBSIMS workstation. The transmission electron microscopy (TEM) characterization was performed using a JEOL 2010 TEM operating at 200 kV.

RESULTS AND DISCUSSION

Formation of Porous InP

Fig. 1 shows the cyclic voltammetric response of an n-InP electrode in a 5 mol dm^{-3} KOH solution. The potential was scanned at a rate of 2.5 mV s^{-1} from 0.0 V to 0.68 V and back to 0.0 V. At potentials less than 0.3 V, very little current flow is observed, but continued anodization to potentials greater than 0.35 V results in a rapid increase in the current density from a value of 1 mA cm^{-2} at 0.35 V to a peak value of 20 mA cm^{-2} at 0.48 V. Above 0.48 V, the current density decreases quite rapidly, reaching a value of 3 mA cm^{-2} at 0.6 V. Clearly, a significant anodic oxidation process occurs above 0.35 V and becomes self-limiting at higher potentials.

Examination of electrode cross-sections using TEM shows that the process corresponding to the anodic current in Fig. 1 involves the formation of a porous sub-
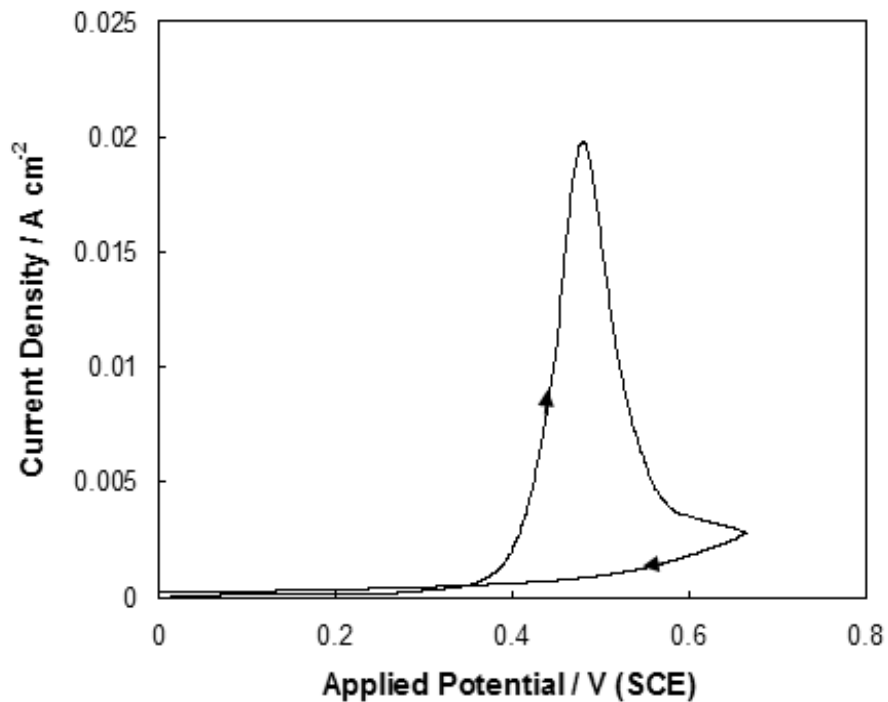
Fig. 1 Cyclic voltamogram of an n-InP electrode in a 5 mol dm^{-3} KOH electrolyte from 0
.0 V to 0.68 V (SCE). The potential was scanned at a rate of 2.5 mV s^{-1}.
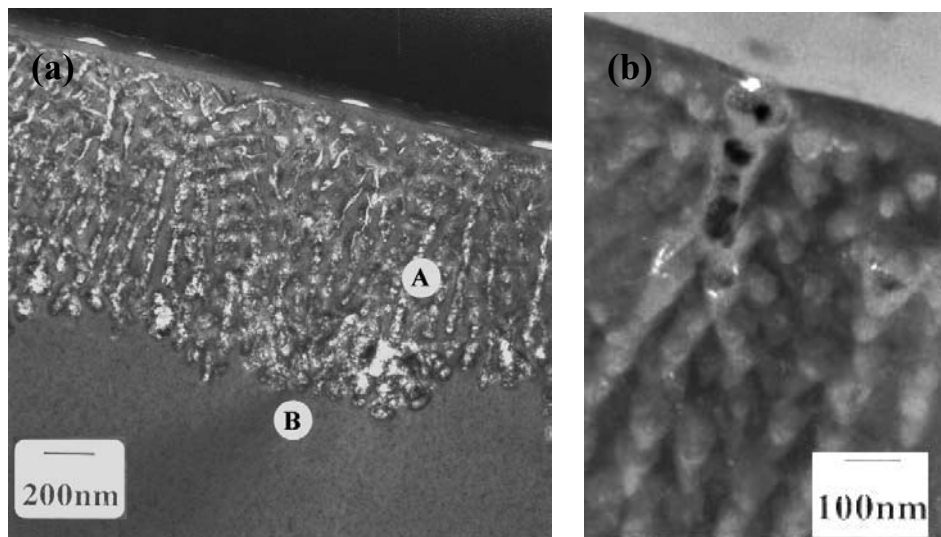

Fig. 2 Cross-sectional bright field through focal TEM of n-InP after a potential sweep
from 0.0 V to 0.7 V (SCE) at a scan rate of 2.5 mV s-1 in 5 mol dm-3 KOH electrolyte.
(b) Dark Field TEM of the porous InP cross-section showing a channel in the near-
surface layer. The plane of the micrographs is (110).

surface region. Fig. 2(a) is a TEM micrograph of a cross-section of an InP electrode after a potential sweep from 0.0 V to 0.7 V in 5 mol dm-3 KOH. The porous region is clearly observed to extend over 1.1 μm into the InP substrate. However, a thin layer ~40 nm in thickness close to the surface appears to be unmodified. We have observed similar behavior under both potential sweep and constant potential conditions in KOH electrolytes [12] with concentrations ranging from 2 – 5 mol dm-3 and in all cases a thin, dense, near-surface layer is present above the porous region. Electron diffraction measurements have shown this layer to be single crystal InP, i.e. unmodified electrode material.

Mechanism

The mechanism by which a porous region can form by electrochemical oxidation of the substrate, despite the presence of this dense InP layer at the surface is not apparent from Fig. 2(a). Closer examination by TEM reveals that the dense, near-surface layer is penetrated at certain points by narrow channels. The TEM micrograph in Fig. 2(b) shows a typical example. This is corroborated by AFM examination of the surface. Fig. 3a shows an AFM image of the surface of an InP electrode that was subjected to a potential sweep from 0.0 V to 0.425 V in 5 mol dm^{-3} KOH at 2.5 mV s^{-1}. The image clearly shows an etch pit which has formed on the surface. Similar pits were observed in AFM images obtained for potential sweep experiments at other upper potentials in the range 0.4 V to 0.53 V. For example, an image obtained for an upper potential of 0.48 V (*i.e.* at the current peak) is shown in Fig. 3b. Line scans through the AFM images in Figs. 3a and 3b are shown in Figs. 3c and 3d. Although the AFM cannot measure the diameter of deep pits, we can obtain some estimate of the diameter of the pits from these traces. Thus, taking the value of the full width at half maximum (FWHM) from these traces we obtain a value of ~50 nm for the pit diameter in each case.

It appears that these surface pits correspond to channels which connect the porous region to the bulk electrolyte. This suggests a mechanism by which the electrochemical oxidation of InP at the pore tips, and thus porous layer growth, can continue. Both the porous layer and the channels through the near-surface layer must be filled with electrolyte. This would enable ionic current to flow and electrochemical oxidation of InP to proceed at the pore tips, thus providing a mechanism by which the porous layer can grow. Consequently, these channels have a critical role in the evolution of the porous structure.

In order to investigate the mechanism by which porosity develops, experiments were carried out in which the potential was swept from 0.0 V to 0.44 V (*i.e.* the potential sweep was stopped when the current reached approximately half its peak value) and the electrode was then cross-sectioned and examined. A TEM micrograph of such a cross-section is shown in Fig. 4. This reveals that, at this stage of the anodization, individual porous areas had formed which had a triangular cross-section with the base of the triangle
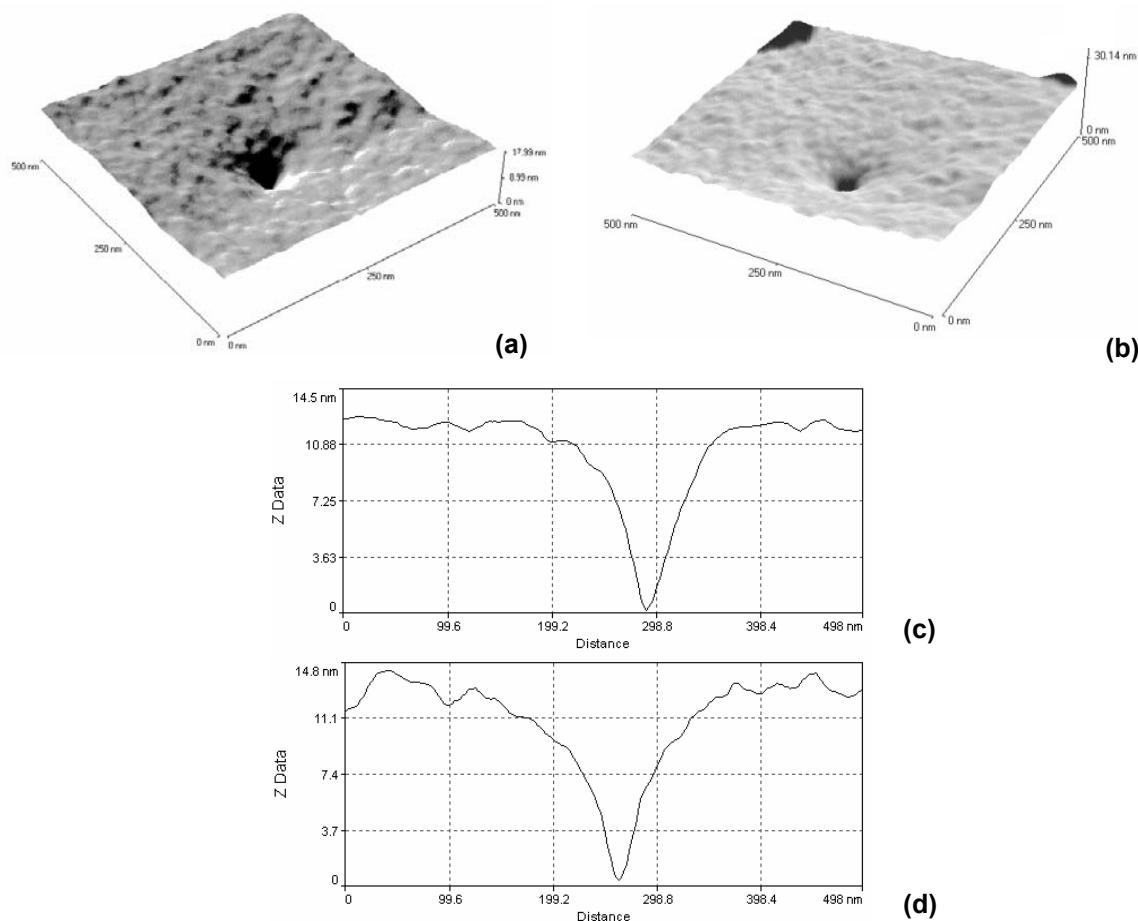
(a)

(b)

(c)

(d)

Fig. 3 AFM images of the InP surface after potential sweep anodization at 2.5 mV s^{-1} in 5 mol dm^{-3} KOH from 0.0 V to (a) 0.425 V, (b) 0.48 V. (c) Line scan of the pore shown in (a); (d) Line scan of the pore shown in (b).

parallel to the InP surface. As was observed for the more fully developed porous layer (Fig. 2) the triangular porous region is separated from the surface by a thin non-porous layer. The measured thickness of this layer in Fig. 4 is ~40 nm. The dimensions of the triangular cross-section in Fig. 4 are shown in Fig. 5. The base of the triangle measures 920 nm and the other sides are equal to each other within experimental error (2%) with a length of 800 nm. Thus, the height of the triangle is 655 nm and the angle between the base and the sides is 54.9^{0}.

The cross-section in Fig. 4 is along the (011) plane. By symmetry we would expect a similar cross-section along the perpendicular (011) plane which suggests that the porous region in Fig. 4 may have a square-based pyramidal structure. This was

investigated by plan-view TEM observation of the electrode. Fig. 6 shows a TEM micrograph of a slice through the InP in the (100) plane, parallel to the surface and ~100 nm below it. A porous region with an approximately square outline is clearly visible, consistent with a square pyramidal structure for the porous region as suggested above.
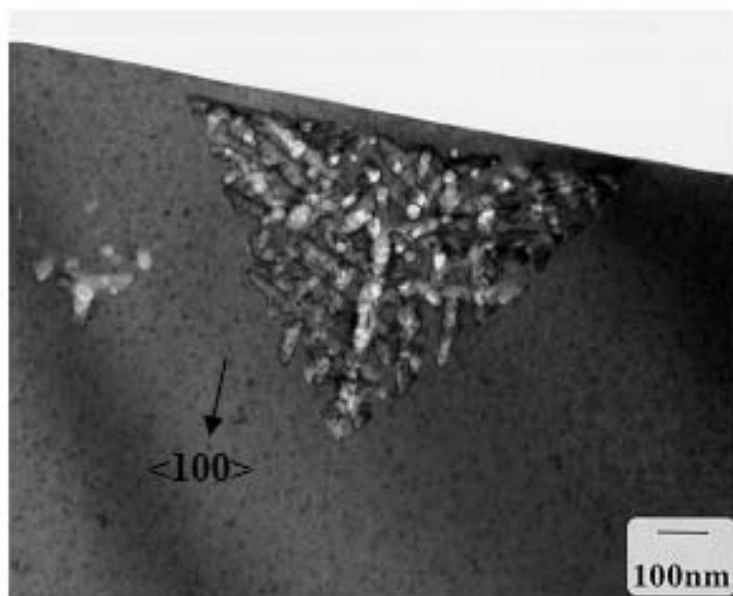

Fig. 4 Bright field TEM of a cross section of an InP electrode after a potential sweep from 0.0 to 0.44 V (SCE) in 5 mol dm^{-3} KOH at 2.5 mV s^{-1}. The plane of the micrograph is (110).
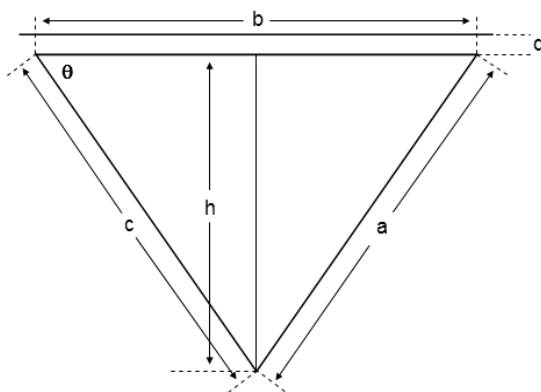

Fig. 5 Schematic representation of the triangular porous region shown in Fig. 4. The base of the triangle is a distance $d = 40$ nm below the surface of the InP. The length of the base is $b = 920$ nm, the length of the sides is $a = c = 800$ nm and the angle between the base and side is $\theta = 54.9^0$.
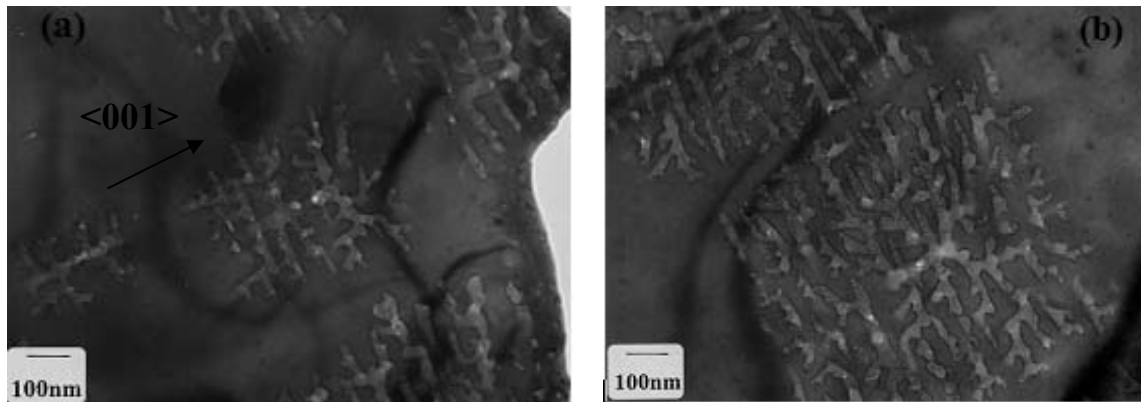
Fig. 6 Plan view bright field TEM images of a section through a porous InP layer ~100 nm below the surface of the electrode. Anodization conditions were the same as in Fig. 4. The plane of the micrograph is (100). Nearby porous domains are visible.

The sides of the square in Fig. 6 are parallel to the <100> direction and are ~800 nm in length. We suggest that each pyramidal porous structure formed corresponds to a single channel through the near-surface layer. We further suggest that the pyramidal structure arises as a result of preferential pore propagation along the <100> directions.

To facilitate discussion of the growth of an individual pyramidal porous structure, we define cartesian co-ordinates as follows. We define a *y*-axis along the [100] direction (*i.e.* normal to the surface of the electrode), an *x*-axis along the [010] direction and a *z*-axis along the [001] direction. The origin (0,0,0) is defined as the bottom of the channel through the near-surface layer. This is depicted in Fig. 7.

Consider a pore propagating from the origin. It can propagate in any of five directions, namely –*y, x,* –*x, z* and –*z*. Assume that the pore is propagating at some linear velocity *v*. If it propagates along the –*y* direction it will reach a point with co-ordinates (0, –*vt*, 0) a distance *vt* below the surface layer at time *t*. Similarly, if it propagates along the *x* direction it will reach a point (*vt*, 0, 0) just underneath the near-surface layer. If the pore propagates for time *t*/2 along the –*y* direction and then branches and travels for time *t*/2 along the *x* direction, it will reach a point (*vt*/2, –*vt*/2, 0) at time *t*. In fact, if the pore propagates along any combination of paths along the –*y* direction and the *x* direction it will reach a point on the line joining (0, –*vt*, 0) and (*vt*, 0, 0). Likewise, a pore propagating by any combination of paths along the –*y* direction and the –*x* direction will reach a point on the line joining (0, –*vt*, 0) and (–*vt*, 0, 0), at time *t*. Similarly, pores propagating along paths involving the –*y* direction in combination with the *z* direction and the –*z* direction will reach, at time *t*, points on the lines joining (0, –*vt*, 0) to (0, 0, *vt*) and (0, 0, –*vt*) respectively. Extending the argument to combinations of paths involving all three axes, it is clear that pores propagating in this way will reach, at time *t*, points on

the surface of a square based pyramid defined by the above-mentioned four line segments and the plane of the bottom of the near-surface layer.
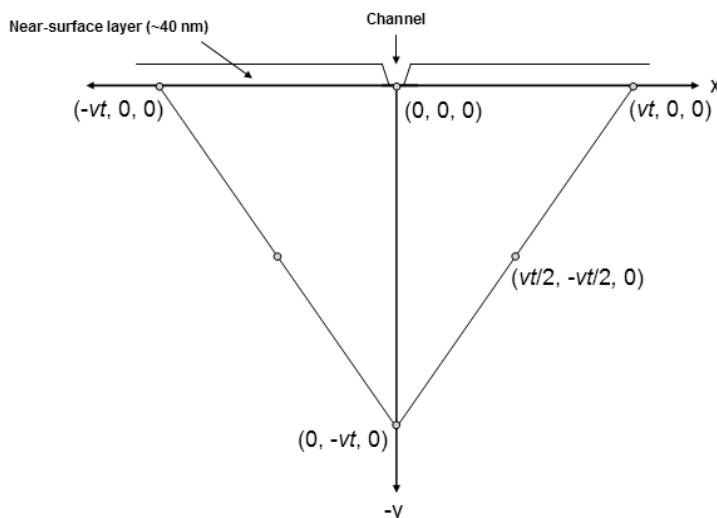

Fig. 7 Definition of cartesian co-ordinates for an individual porous region. The *y*-axis is normal to the electrode surface and the *z*-axis is out of the plane of the page. The origin is at the bottom of a channel through the near-surface layer as shown.

Density of Surface Pits

Estimates were made of the areal density of pits on electrode surfaces after anodization under potentiodynamic conditions. A series of experiments was carried out in which electrodes were subjected to potential sweeps at 2.5 mV s^{-1} from 0.0 V to upper potentials in the range 0.48 V to 0.68 V and 10 μm × 10 μm AFM images of the resulting surfaces were obtained. A typical such image is shown in Fig. 8 for an upper potential of 0.48 V (corresponding to the current peak). At this lower magnification, multiple pits are visible on the surface. By counting the pits (~23 for this image) in such images we can estimate the average areal density of pits in the surface.

Estimates of pit density were similarly obtained for other upper potentials and the results are plotted in Fig. 9. It is clear that the density of pits in the surface increases progressively with increasing potential. The rate of increase is greatest in the vicinity of 0.45 V. This corresponds to half the peak current on the low-potential side of the peak in the current-voltage curve in Fig. 1a. Above ~0.48 V (*i.e.* the potential of peak current) the pit density begins to plateau and any further increase in pit density is small. Thus, the observed increase in density of pits in Fig. 9 corresponds to the onset of the anodic peak in Fig. 1. As discussed earlier a square based pyramidal porous domain forms beneath
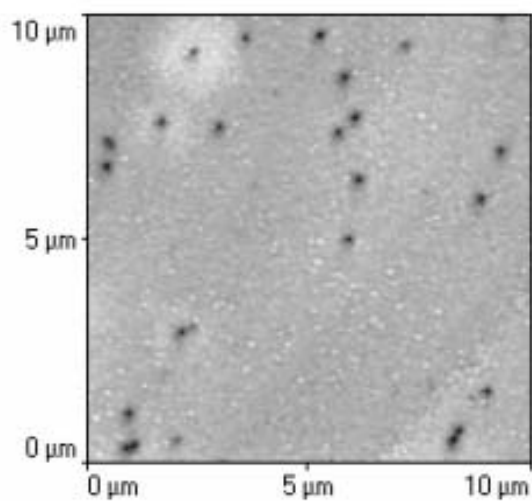
Fig. 8 AFM image of the surface of an InP electrode subjected to a potential sweep from 0.0 V to 0.48 V at 2.5 mV s^{-1} in 5 mol dm^{-3} KOH.
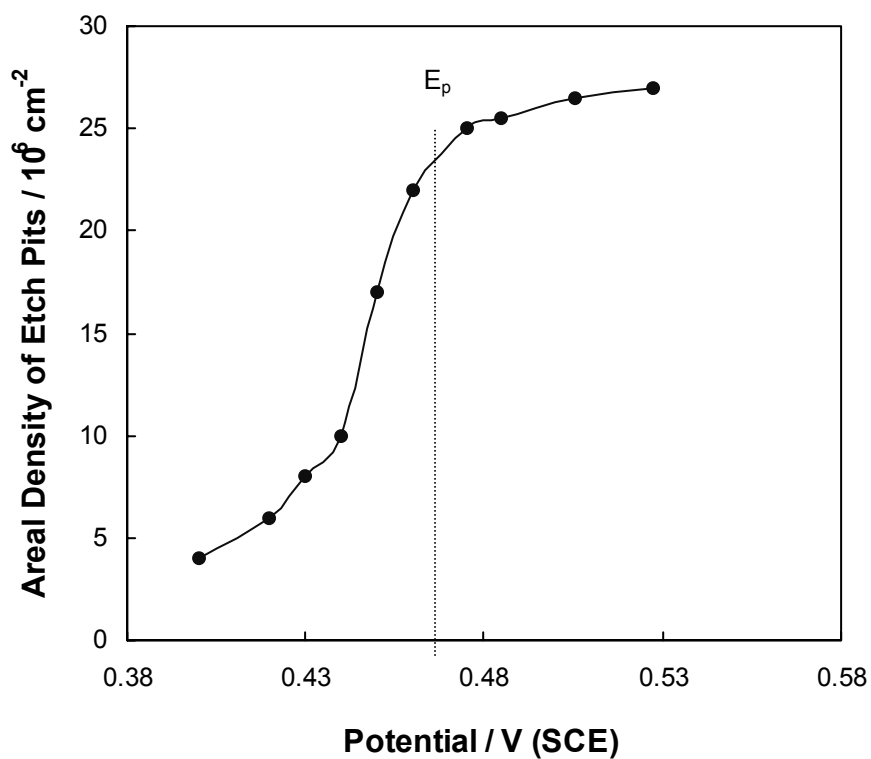

Fig. 9 Surface pit density, as determined by AFM, plotted as a function of the upper potential limit of the potential sweep. The scan rate was 2.5 mV s^{-1} and the electrolyte was 5 mol dm^{-3} KOH.

each etch pit on the surface. Thus, as the etch pits form progressively on the surface of the electrode, so the formation of porous domains also occurs progressively. The progressive formation of square-based pyramidal shaped porous domains beneath etch pits on the surface can be seen in the (100) plan view TEM images in Fig. 10. This plan-view TEM micrograph was acquired after ion-milling ~100 nm into the surface of an InP electrode subjected to a potential sweep from 0.0 V to 0.44

When the domains grow, the current density increases correspondingly. Eventually domains meet, the interface between the porous and bulk regions of InP becomes relatively flat and its total effective surface area decreases resulting in a decrease in current density. Numerical models of this process are being developed and preliminary results are reported in another paper in this proceedings volume.
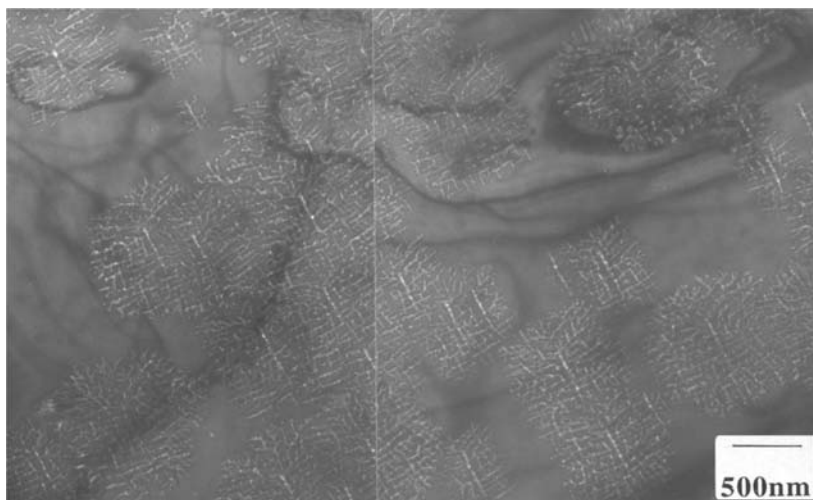

Fig. 10 Plan view TEM of n-InP ~100 nm below the surface after a potential sweep from 0.0 V to 0.44 V at a scan rate of 2.5 mV s^{-1} in 5 mol dm^{-3} KOH electrolyte. The progressive development of the porous domains is apparent.

Potentiostatic Anodization

Experiments were also carried out at constant potential. In a series of experiments in 5 mol dm^{-3} KOH, the potential was stepped from open circuit to potential values in the range 0.5 – 0.75 V. These potentials correspond to values on a typical current-voltage curve at which porous layer formation is observed. Fig. 11 shows the current-time curve obtained for an InP electrode anodized in 5 mol dm^{-3} KOH at a potential of 0.5 V. The current initially increases with time reaching a peak after 23 s and subsequently decreases. This type of current-time curve is typically observed where a nucleation process is occurring. Similar current-time curves are observed for InP electrodes anodized in 2 and 3 mol dm^{-3} KOH and details of these can be found elsewhere. [12] In all cases, porous layers are observed to form beneath the surface.

Cross-sectional TEM examination was carried out on electrodes anodized at constant potentials of 0.5 V, 0.6 V and 0.75 V respectively. The images obtained are shown in Fig. 12. In each case, it is clear that a porous region has been formed beneath a thin near-surface layer, as was observed under potentiodynamic conditions.

AFM studies were also conducted on electrode surfaces subjected to potentiostatic anodization. Values of pit density obtained from images corresponding to various times along the curve in Fig. 11 are plotted in Fig. 13. It is observed that the density of pits formed on the surface increases with time and approaches a plateau value after 20 – 30 s. Thus, surface pitting at constant potential develops in a similar manner to that observed under potential sweep conditions and is a progressive process.
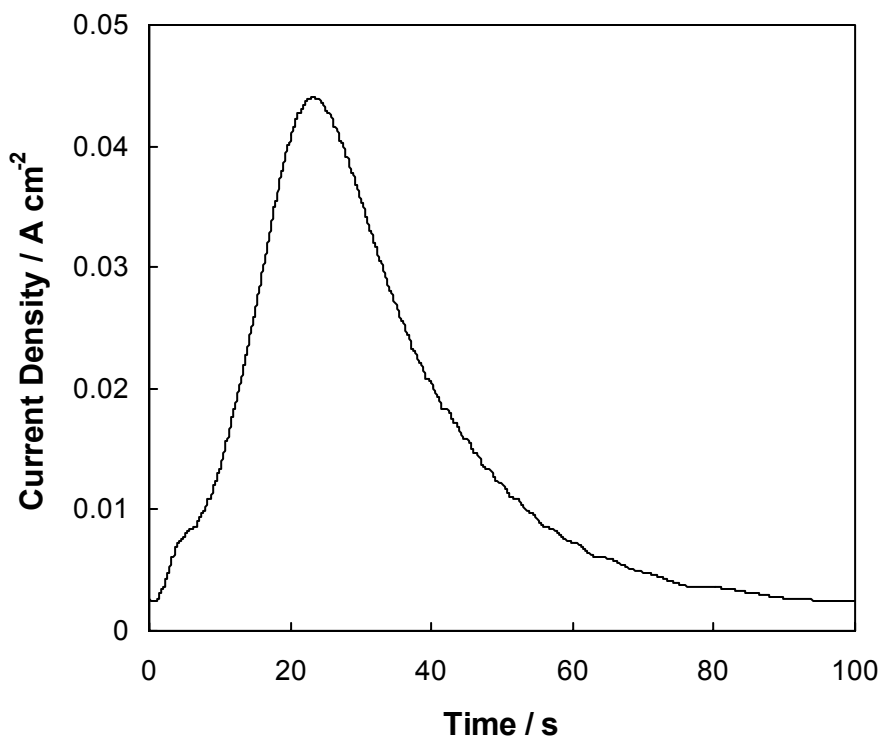

Fig. 11 Current-time curve for InP anodized at a potential of 0.5 V in 5 mol dm^{-3} KOH.
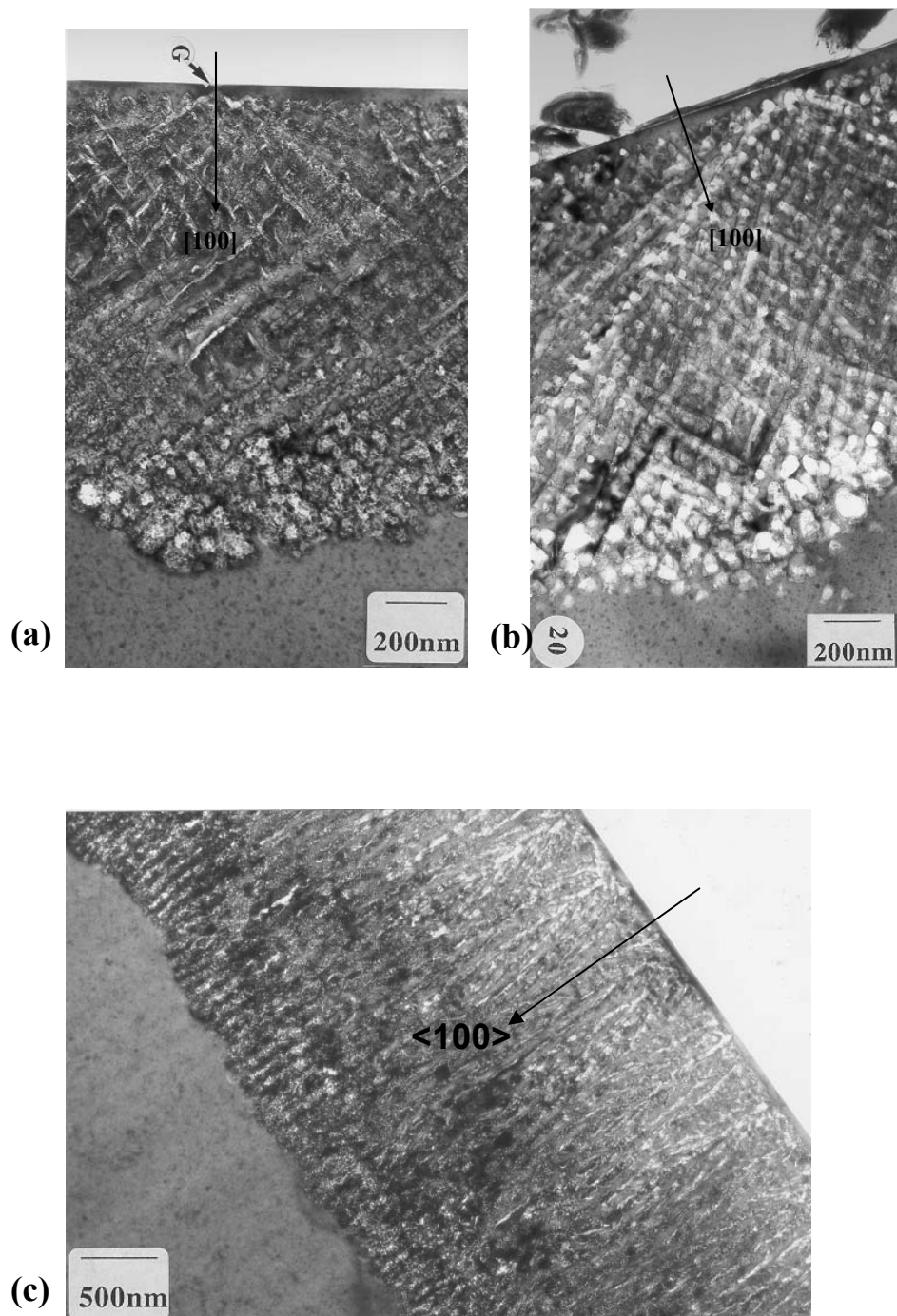
Fig. 12 Cross-sectional bright field through focal TEM micrographs of n-InP after constant potential anodization at (a) 0.5 V, (b) 0.6 V and (c) 0.75 V (SCE) for 100 s in 5 mol dm^{-3} KOH. The plane of the micrographs is (011).
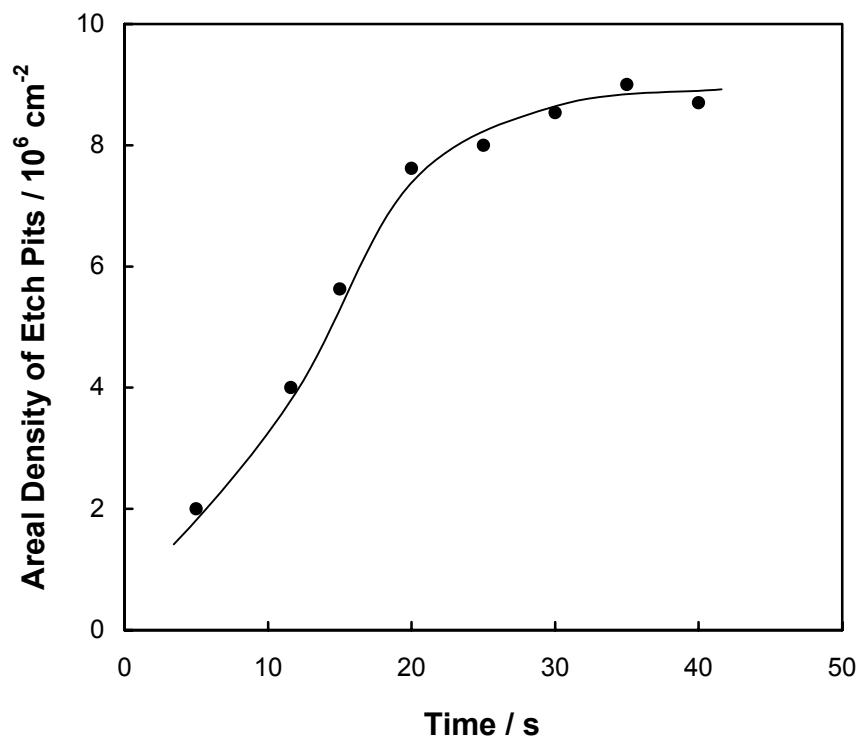
Fig. 13 Surface pit density plotted as a function of time. The data was acquired on multiple areas (10 μm × 10 μm) on multiple electrode surfaces anodized at 0.5 V in 5 mol dm^{-3} KOH.

CONCLUSIONS

At the earlier stages of the anodic formation of porous InP in 5 mol dm^{-3} KOH, TEM clearly shows individual porous domains which appear triangular in cross-section and square in plan view. The cross-sections also show that the domains are separated from the surface by a ~40 nm thick, dense InP layer. It is concluded that the porous domains have a square-based pyramidal shape and that each one develops from an individual surface pit which forms a channel through this near-surface layer. We suggest that the pyramidal structure arises as a result of preferential pore propagation along the <100> directions. It is clear that pores propagating in this way with uniform instantaneous growth rate will reach, at a given time, points on the surface of a square-based pyramid. AFM measurements show that the density of surface pits increases with time. Each of these pits acts as a source for a pyramidal porous domain, and these domains eventually form a continuous porous layer. This implies that the development of porous domains beneath the surface is also progressive in nature. Evidence for this is

seen in plan view TEM images in which domains in different areas of the same surface are seen to be at different stages of development. When the domains grow, the current density increases correspondingly. Eventually domains meet, the interface between the porous and bulk InP becomes relatively flat and its total effective surface area decreases resulting in a decrease in the current density. Quantitative models of this process are being developed. Experiments were also carried out at constant potential values in the range 0.5 – 0.75 V. The current was observed to increase with time reaching a peak (e.g., at 23 s for 0.5 V) and subsequently decrease. In all cases, porous layers are observed to form beneath the electrode surface. It was observed that the density of pits formed on the surface increases with time and approaches a plateau value (after 20 – 30 s in the case of 0.5 V). Thus, surface pitting at constant potential develops in a similar manner to that observed under potential sweep conditions and is a progressive process.

REFERENCES

[1] L.T. Canham, *Appl. Phys. Lett.*, **57**, 1046 (1990)

[2] H. Föll, *Appl. Phys. A*, **53**, 8 (1991)

[3] T. Holec, T. Chvojka, I. Jelínek, J. Jindřich, I. Němec, I. Pelant, J. Valenta and J. Dian, *Mater. Sci. Eng. C*, **19**, 251 (2002)

[4] R.J. Martín-Palma, J.M. Martínez-Duart, L. Li and R.A. Levy, *Mater. Sci. Eng. C,* **19**, 359 (2002)

[5] A. Matoussi, T. Boufaden, A. Missaoui, S. Guermazi, B. Bessaïs, Y. Mlik and B. El Jani, *Microelectronics Journal,* **32**, 995 (2001)

[6] A. Jain, S. Rogojevic, S. Ponoth, N. Agarwal, I. Matthew, W.N. Gill, P. Persans, M. Tomozawa, J.L. Plawsky and E. Simonyi, *Thin Solid Films,* **398**, 513 (2001)

[7] N.E. Chayen, E. Saridakis, R. El-Bahar, Y. Nemirovsky, *J. Molec. Biol.,* **312**, 591 (2001)

[8] S. Langa, J. Carstensen, M. Christophersen, H. Föll, and I.M. Tiginyanu, *Appl. Phys. Lett.*, **78**, 1074 (2001)

[9] G. Oskam, A. Natarajan, P.C. Searson and F.M. Ross, *Appl. Surf. Sci.*, **119**, 160 (1997)

[10] M.M. Faktor, D.G. Fiddyment and M.R. Taylor, *J. Electrochem. Soc.*, **122**, 1566 (1975)

[11] F.M. Ross, G. Oskam, P.C. Searson, J.M. Macaulay and J.A. Liddle, *Philos. Mag. A*, **75**, 2 (1997)

[12] C. O'Dwyer, D.N. Buckley, V.J. Cunnane, D. Sutton, M. Serantoni and S.B. Newcomb, in *Proceedings of the State-of-the-Art Program on Compound Semiconductors XXXVII*, PV 2002-14, p. 259, The Electrochemical Society, Proceedings Series, Pennington, NJ (2002)

[13] S. Langa, J. Carstensen, I.M. Tiginyanu, M. Christophersen and H. Föll, *Electrochem. Solid-State Lett.*, **4**, G50 (2001)

[14] S. Langa, I.M. Tiginyanu, J. Carstensen, M. Christophersen and H. Föll, *Electrochem. Solid-State Lett.* **3**, 514 (2000)

[15] E. Harvey, C. O'Dwyer, T. Melly, D.N. Buckley, V.J. Cunnane, D. Sutton, S.B. Newcomb and S.N.G. Chu, in *Proceedings of the 35th State-of-the-Art Program on Compound Semiconductors*, P.C. Chang, S.N.G. Chu, and D.N. Buckley, Editors, PV 2001-2, p. 87, The Electrochemical Society, Proceedings Series, Pennington, NJ (2001)

[16] P. Schmuki, J. Fraser, C.M. Vitus, M.J. Graham, H.S. Isaacs, *J. Electrochem. Soc.*, **143**, 3316 (1996)

[17] P. Schmuki, D.J. Lockwood, J. Fraser, M.J. Graham, H.S. Isaacs, *Mater. Res. Soc. Symp. Proc.,* **431**, 439 (1996)

[18] M. Christopherson, J. Carstensen, A. Feuerhake and H. Föll, *Mater. Sci. Eng. B*, **69**, 70, 194 (2000)

[19] S. Rönnebeck, J. Carstensen, S. Ottow and H. Föll, *Electrochem. Solid-State Lett.*, **2**, 126 (1999)

[20] P. Schmuki, L.E. Erickson, D.J. Lockwood, J.W. Fraser, G. Champion, H.J. Labbé, *Appl. Phys. Lett.*, **72,** 1039 (1998)

[21] B.H. Erne, D. Vanmaekelbergh and J.J. Kelly, *J. Electrochem. Soc.*, **143**, 305 (1996)

[22] J. Carstensen, M. Christophersen and H. Föll, *Mater. Sci. Eng., B*, **69-70**, 23 (2000)

[23] S. Langa, J. Carstensen, I.M. Tiginyanu, M. Christophersen and H. Föll, *Electrochem. Solid-State Lett.*, **5**, C14 (2002)